Engine On/Off Control for Dimensioning Hybrid Electric Powertrains via Convex Optimization

Nikolce Murgovski, Lars Mårdh Johannesson, *Member, IEEE*, and Jonas Sjöberg, *Member, IEEE*

***Abstract*—This paper presents a novel heuristic method for optimal control of mixed-integer problems that, for given feasible values of the integer variables, are convex in the rest of the variables. The method is based on Pontryagin's maximum principle and allows the problem to be solved using convex optimization techniques. The advantage of this approach is the short computation time for obtaining a solution near the global optimum, which may otherwise need very long computation time when solved by algorithms guaranteeing global optimum, such as dynamic programming (DP). In this paper, the method is applied to the problem of battery dimensioning and power split control of a plug-in hybrid electric vehicle (PHEV), where the only integer variable is the engine on/off control, but the method can be extended to problems with more integer variables. The studied vehicle is a city bus, which is driven along a perfectly known bus line with a fixed charging infrastructure. The bus can charge either at standstill or while driving along a tramline (slide in). The problem is approached in two different scenarios: First, only the optimal power split control is obtained for several fixed battery sizes; and second, both battery size and power split control are optimized simultaneously. Optimizations are performed over four different bus lines and two different battery types, giving solutions that are very close to the global optimum obtained by DP.**

***Index Terms*—Battery sizing, convex optimization, plug-in/slide-in hybrid electric vehicle (HEV), Pontryagin's maximum principle, power management.**

I. Introduction

In addition to internal combustion engines (ICEs), hybrid electric vehicles (HEVs) have an energy buffer, typically a battery and/or a supercapacitor, and one or more electric machines (EMs). This gives them an additional degree of freedom compared with conventional vehicles, which allows for a more efficient operation, due to the possibility to recover braking energy by using the EMs as generators and by storing the energy in the buffer, the ability to shut down the ICE during idling and low load demands, and the possibility to run the ICE at more efficient load conditions while storing the excess energy in the buffer. (For a detailed overview on hybrid vehicles, see, e.g., [1].)

Plug-in HEVs (PHEVs) have in addition a charging connector, which allows them to draw electric energy from the grid. The PHEVs that are being considered in public transport are designed to charge from fast-charge docking stations while standing still at stops along the bus line [2] and while driving along sections on the bus line [3], [4]. In [3], the PHEV city bus is inductively charged from underground cables that have been buried along sections of the bus line. In [4], the PHEV, which is a dual-mode trolley bus, can draw electricity from overhead wires along sections of existing tramlines. Throughout this paper, the charge-while-driving sections of the bus line will be called slide-in intervals.

To be cost effective, the PHEV city bus is preferred to drive a significant part of the bus line on electric power, although the charging intervals might be short, and the charging infrastructure might be sparsely distributed. This puts hard constraints on the sizing of the energy buffer, i.e., determining power rating and energy capacity, which is not only dependent on the charging infrastructure but also on the drive patterns, the topography along the bus line, and varying factors, such as fuel and electricity prices. Moreover, a complicating issue when evaluating HEV city buses is that the energy efficiency of the powertrain depends on how well adapted the energy management strategy (power split control) is to the bus line [5]. For PHEV city buses, the energy management strategy decides the operating point of the ICE and thereby when and at which rate the energy buffer is to be discharged. When optimizing the PHEV public transportation system based on a dynamic model of the powertrain, a badly designed/adjusted energy management may lead to a nonoptimal size of the energy buffer [6]. Hence, to overcome this problem, both the size of the energy buffer and the energy management need to be optimized simultaneously.

The problem of optimal sizing and control of HEVs is traditionally solved by dynamic programming (DP) [7], for which a vast number of scientific articles are available [8]–[13]. The main advantage with DP is the capability to use nonlinear nonconvex models of the components consisting of continuous and integer (mixed-integer) optimization variables. However, a serious limitation of DP is that computation time exponentially increases with the number of state variables [7]. As a

Manuscript received March 19, 2012; revised October 5, 2012 and November 29, 2012; accepted February 20, 2013. Date of publication March 8, 2013; date of current version September 11, 2013. This work was supported in part by the Swedish Energy Agency. The review of this paper was coordinated by Dr. M. Kazerani.

N. Murgovski and J. Sjöberg are with the Department of Signals and Systems, Chalmers University of Technology, 41296 Gothenburg, Sweden. (e-mail: nikolce.murgovski@chalmers.se; jonas.sjoberg@chalmers.se).

L. M. Johannesson is with the Department of Signals and Systems, Chalmers University of Technology, 41296 Gothenburg, Sweden, and also with Viktoria Swedish ICT, SE-417 56 Gothenburg, Sweden (e-mail: larsjo@chalmers.se; lars.johannesson@viktoria.se).

Color versions of one or more of the figures in this paper are available online at http://ieeexplore.ieee.org.

Digital Object Identifier 10.1109/TVT.2013.2251920

consequence, the powertrain model is typically limited to only one, or possibly two, continuous state variables. Moreover, since DP operates by recursively solving a smaller subproblem for each time step, the second limitation of DP is that it is not possible to include directly the component sizing into the optimization. Instead, DP must be run in several loops to obtain the optimal control over a grid of component sizes, which further increases computation time.

Another approach, which is proposed in [14], uses convex optimization for optimal control of HEVs. In this early study, the powertrain components are expressed with linear models, and the optimization problem is a linear program. In a more recent study [15], the strategy has been extended to powertrains with quadratic losses for the components, and not only optimal control is obtained but also, simultaneously, the energy buffer is sized by solving a semidefinite convex program [16]. The study showed that, for a battery with nearly constant voltage within the allowed state-of-charge (SOC) interval, the error due to convexifying approximations of the powertrain components is small. However, the disadvantage of this strategy is that it relies on heuristic decision for the integer variables, such as gear, and engine on/off.

This paper is an extension of [15] and proposes a novel heuristic strategy that decides engine on/off control for PHEV powertrains in series topology [1]. The strategy is based on Pontryagin's maximum principle [17] and requires iteratively solving the convex problem while using the Hamiltonian [18], [19] to obtain information on the possible improvement in cost from flipping the value of the engine on/off signal at certain time instances. This paper shows several examples where the problem of cost optimal battery sizing, which is investigated for four different bus lines and two different battery types, is solved in less than 17 min in a PC. The results are validated with DP showing less than 0.35% difference from the global optimum. Moreover, to test the convergence of the algorithm, the problem of optimal control of a powertrain with a fixed battery is solved for 176 different battery sizes. Each optimization needed less than 5 min and achieved a solution within 0.03% of the global optimum.

This paper is outlined as follows. Problem formulation and modeling details are described in Section II. Convex modeling and the lower bound on the optimization problem are discussed in Section III. A novel heuristic algorithm is depicted in Section IV. Examples of optimal battery sizing are given in Section V. Finally, this paper is ended with discussion and conclusion in Sections VI and VII, respectively.

II. Problem Formulation

Here, we give the background on the bus line and vehicle model, and we formulate the PHEV battery sizing and the power split control problem.

A. Bus Line and Vehicle Model

The investigated vehicle is a slide-in/plug-in hybrid electric bus in a series powertrain topology [1], where unlike the conventional vehicles, its combustion engine is completely

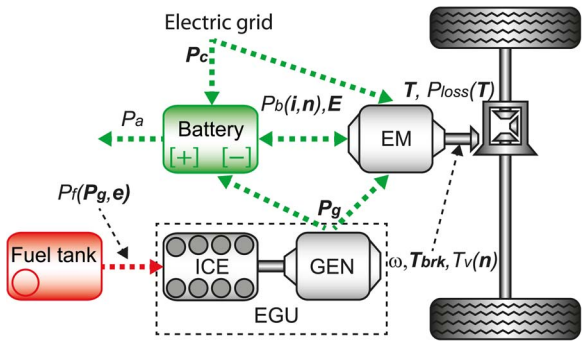

Fig. 1. Series PHEV powertrain model.

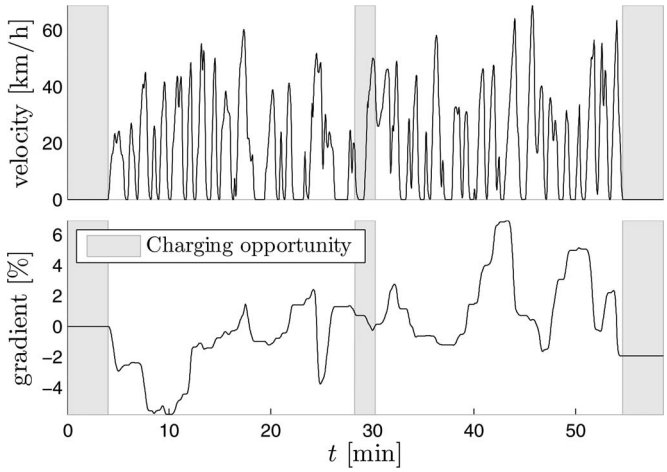

Fig. 2. Bus line model described by demanded velocity and road gradient. The bus line has three charging opportunities, which are shaded in the figure. The bus can charge for 4 min while standing still at each end and for 2 min while driving along a tramline at about the middle of the bus line.

decoupled from the wheels (see Fig. 1). The wheels are propelled by an EM that receives energy from the electric grid, the battery, and the engine–generator unit (EGU).

The bus is driven on a bus line described by a road gradient and demands velocity at each point of time (see Fig. 2). The bus line model, together with the vehicle inertia, aerodynamic drag and rolling resistance, can be turned into torque $T_v(\boldsymbol{n}, t)$ and speed $\omega(t)$ demanded by the EM. The EM, which has torque $\boldsymbol{T}(t)$ (to improve readability, decision variables will be marked in bold), is designed to be able to deliver the demanded torque, except during braking when not all torque may be recuperated to charge the battery, but some portion $\boldsymbol{T}_{\mathbf{brk}}(t) \geq 0$ is dissipated at the friction brakes, i.e.,

$$\boldsymbol{T}(t) = T_v(\boldsymbol{n}, t) - \boldsymbol{T}_{\mathbf{brk}}(t). \tag{1}$$

The model considers a demanded torque $T_v(\boldsymbol{n}, t)$ that is an affine function on battery mass; hence, it is affine on the number of battery cells $\boldsymbol{n}$. A detailed description of $T_v(\boldsymbol{n}, t)$ is given in Appendix A.

The powertrain electric path is described by a power balance

$$\boldsymbol{T}(t)\omega(t) + P_{\text{loss}}\left(\boldsymbol{T}(t), t\right) = P_b\left(\boldsymbol{i}(t), \boldsymbol{n}\right) + \boldsymbol{P_g}(t)\boldsymbol{e}(t) + \boldsymbol{P_c}(t)c(t) - P_a \tag{2}$$

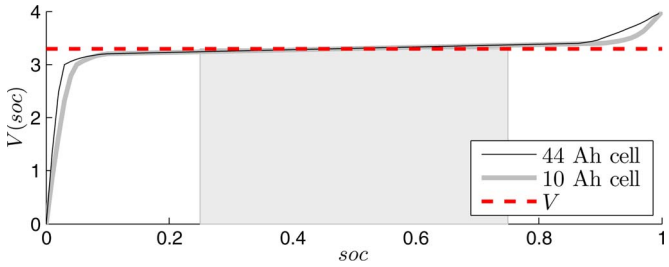

Fig. 3. Model of the battery open circuit voltage. The solid lines represent the original models, and the dashed line is the approximation. A good fit is expected in the allowed SOC range represented by the shaded region.

that relates the EM electric power, at the left side of the equality, to battery power $P_b(\boldsymbol{i}(t), \boldsymbol{n})$, EGU power $\boldsymbol{P}_g(t)$, grid charging power $\boldsymbol{P}_c(t)$, and power consumed by auxiliary devices P_a. The losses of the EM, including the losses of the power electronics, are modeled as a quadratic function on $\boldsymbol{T}(t)$ as follows:

$$P_{\text{loss}}\left(\boldsymbol{T}(t),\, t\right) = b_0\left(\omega(t)\right)\boldsymbol{T^2}(t) + b_1\left(\omega(t)\right)\boldsymbol{T}(t) + b_2\left(\omega(t)\right)$$

with speed-dependent coefficients, where $b_j(\omega(t)) \geq 0,\ j \in \{0, 2\}\ \forall t \in [t_0, t_f]$. The EGU losses are also modeled by the following quadratic function:

$$P_f\left(\boldsymbol{P_g}(t), \boldsymbol{e}(t)\right) = \left(a_0\boldsymbol{P_g^2}(t) + a_1\boldsymbol{P_g}(t) + a_2\right)\boldsymbol{e}(t) \quad (3)$$

with $a_j \geq 0, j \in \{0, 2\}$, where $\boldsymbol{e}(t)$ is a binary signal that is needed to allow zero fuel power, i.e., to remove the idling losses a_2 when the engine is off. More details on the validity of the EM and EGU models can be found in [15].

The vehicle has three charging opportunities, i.e., 4 min while standing still at each end, and 2 min while *sliding in* a tramline at about the middle of the bus line. It is assumed, for simplicity, that the chargers have equal maximum power $P_{c,\max}$ and constant charging efficiency η. The charging opportunities, shaded in Fig. 2, are indicated by binary signal $c(t)$.

B. Battery Model

The battery consists of $\boldsymbol{n}$ identical cells equally divided into parallel strings, with the strings constructed of cells connected in series. In this paper, two types of cells are considered: a high-energy 44-Ah cell and a high-power 10-Ah cell. The cells' open circuit voltage, which is shown in Fig. 3, is approximated by a constant voltage V, for simplicity. This gives a good fit within the operating state-of-charge (SOC) range of the batteries, but the method presented in this paper can also be applied to batteries with affine voltage–SOC approximation (details on convex modeling can be found in [20]).

Denoting the cell current and resistance by $\boldsymbol{i}_c(t)$ and R, respectively, the battery pack power can be expressed as

$$P_b\left(\boldsymbol{i_c}(t),\, \boldsymbol{n}\right) = \left(V\boldsymbol{i_c}(t) - R\boldsymbol{i_c^2}(t)\right)\boldsymbol{n} \quad (4)$$

showing that the power of each cell $P_b(\boldsymbol{i}_c(t),\, \boldsymbol{n})/\boldsymbol{n}$ is equal and does not depend on the configuration of cells (series/parallel). Therefore, the main objective of this paper is to determine the total number of cells in the pack. After the optimal number of cells is obtained, the cells can be configured in parallel strings such that the open circuit voltage of a string fulfills a desired specification. It can be expected that the error due to rounding the total number of cells to a multiple of the number of cells in series will be small if the results point to a large number of cells. This will be generally the case if the cells are chosen with very small capacity as it can be assumed that each cell is constructed by connecting smaller cells in parallel. With this reasoning, the cells can be chosen to be small enough to consider $\boldsymbol{n}$ as a real-valued variable. (Then, the optimal number of cells can also be interpreted as the optimal pack capacity.)

This paper studies two scenarios with $\boldsymbol{n}$ considered as an integer or as a real number. It has been shown in [15] that, when $\boldsymbol{n}$ has a real value, it is beneficial to replace the cell current in (4) with the pack current $\boldsymbol{i}(t) = \boldsymbol{n}\boldsymbol{i}_c(t)$, giving the following battery power equation:

$$P_b\left(\boldsymbol{i}(t), \boldsymbol{n}\right) = V\boldsymbol{i}(t) - R\frac{\boldsymbol{i^2}(t)}{\boldsymbol{n}}. \quad (5)$$

This replaces the nonconvex product of two variables $\boldsymbol{i}_c(t)\boldsymbol{n}$ in (4) by a quadratic-over-linear function $\boldsymbol{i}^2(t)/\boldsymbol{n}$ that is convex in both $\boldsymbol{i}$ and $\boldsymbol{n}$ for the $\boldsymbol{n}$ real and strictly positive number.

Using pack current $\boldsymbol{i}(t)$, the battery dynamics can be described by

$$\dot{\boldsymbol{E}}(t) = -V\boldsymbol{i}(t)$$

where $\boldsymbol{E}(t)$ is the pack energy.

C. Mixed-Integer Optimization Problem

The studied optimization problem is formulated to minimize the operational and component costs. The component cost is a linear function on battery cells, i.e., $w_b\boldsymbol{n}$, whereas the operational cost refers to the cumulative use of fuel and electricity on the bus line, which at each time instant can be represented as

$$J\left(\boldsymbol{P_g}(t), \boldsymbol{P_c}(t), \boldsymbol{e}(t)\right) = w_f P_f\left(\boldsymbol{P_g}(t), \boldsymbol{e}(t)\right) + \frac{w_c}{\eta}\boldsymbol{P_c}(t). \quad (6)$$

The coefficients w_b [currency] and w_f, w_c [currency/kWh] are used to transform the two costs into a single unit.

The optimization problem can be then summarized as the following nonlinear mixed-integer minimization problem:

minimize

$$\int_{t_0}^{t_f} J\left(\boldsymbol{P}_g(t), \boldsymbol{P}_c(t), \boldsymbol{e}(t)\right) dt + w_b\boldsymbol{n} \quad (7a)$$

subject to $\forall t \in [t_0, t_f]$

$$\boldsymbol{T}(t) \geq \max\left\{T_{\min}\left(\omega(t)\right), T_v(\boldsymbol{n}, t)\right\} \quad (7b)$$

$$\boldsymbol{T}(t)\omega(t) + P_{\text{loss}}\left(\boldsymbol{T}(t), t\right) \leq P_b\left(\boldsymbol{i}(t), \boldsymbol{n}\right) + \boldsymbol{P}_g(t)\boldsymbol{e}(t) + \boldsymbol{P}_c(t)c(t) - P_a \quad (7c)$$

$$\boldsymbol{i}(t) \in [i_{c,\min}, i_{c,\max}]\boldsymbol{n} \quad (7d)$$

$$\boldsymbol{P}_g(t) \in [0, P_{g,\max}] \tag{7e}$$

$$\boldsymbol{P}_c(t) \in [0, \eta P_{c,\max}] \tag{7f}$$

$$\dot{\boldsymbol{E}}(t) = -V\boldsymbol{i}(t) \tag{7g}$$

$$\boldsymbol{E}(t) \in [\mathrm{soc}_{\min}, \mathrm{soc}_{\max}]QV\boldsymbol{n} \tag{7h}$$

$$\boldsymbol{E}(t_f) = \boldsymbol{E}(t_0) = \mathrm{soc}_0 QV\boldsymbol{n} \tag{7i}$$

$$\boldsymbol{e}(t) \in \{0, 1\} \tag{7j}$$

$$\boldsymbol{n} > 0 \tag{7k}$$

$$\boldsymbol{n} \in \begin{cases} \mathbb{Z}, & \text{in scenario where } \boldsymbol{n} \text{ is an integer number} \\ \mathbb{R}, & \text{in scenario where } \boldsymbol{n} \text{ is a real number} \end{cases} \tag{7l}$$

$$\boldsymbol{P}_g(t), \boldsymbol{P}_c(t), \boldsymbol{T}(t), \boldsymbol{E}(t), \boldsymbol{i}(t) \in \mathbb{R} \tag{7m}$$

where $\boldsymbol{P}_g(t)$, $\boldsymbol{P}_c(t)$, $\boldsymbol{T}(t)$, $\boldsymbol{E}(t)$, $\boldsymbol{e}(t)$, $\boldsymbol{i}(t)$, and $\boldsymbol{n}$ are optimization variables. In the view of optimal control, which will be further discussed in Section IV, $\boldsymbol{P}_g(t)$, $\boldsymbol{P}_c(t)$, $\boldsymbol{T}(t)$, $\boldsymbol{e}(t)$, and $\boldsymbol{i}(t)$ are control signals; $\boldsymbol{E}(t)$ is a state; and $\boldsymbol{n}$ is a design parameter. The optimization includes bounds on the cell current, i.e., $i_{c,\min}$ and $i_{c,\max}$; maximum EGU power $P_{g,\max}$; initial SOC soc_0; allowed SOC range $\mathrm{soc}_{\min}$, $\mathrm{soc}_{\max}$; and a speed-dependent bound on the EM generating torque $T_{\min}(\omega(t))$. The battery cell capacity is denoted by Q, and the optimization requires charge sustaining operation by (7i). The initial and final time of the bus line are denoted by t_0 and t_f, respectively.

It can be noticed that (1) and (2) have been relaxed with inequalities in (7b) and (7c), and the braking torque has been taken outside the optimization problem. The reason for doing this will become clear in Section III, but at the moment, we claim that, although the relaxation does change the optimization problem, it does not change the optimal result. Namely, in (7c), the battery and the generator are allowed to produce more power than the electrical power needed by the EM to drive the bus. Similarly, (7b) allows the EM to generate more mechanical power than needed. It is obvious that, at the optimum, these constraints will hold with equality since, otherwise, energy will be wasted unnecessarily. The only exception is during braking when (7b) can be satisfied with inequality, only if the optimal battery is small, and the brake recuperation power is limited by the battery through (7d), rather than by the EM. In either case of bounded recuperation power, the friction brakes will be used to compensate for the remaining braking power. Hence, after the optimization is finished, the optimal braking power can be directly derived from (1) and (2).

The battery dimensioning problem in this paper is approached in two different scenarios. In the first scenario, variable $\boldsymbol{n}$ is taken outside the optimization, such that the mixed-integer optimal control problem (7) is solved over a grid of fixed battery sizes. The disadvantage of this scenario is the long computation time due to the iterative solution of the optimal control problem.

In the second scenario, $\boldsymbol{n}$ is considered a real number, and in (7), the battery is simultaneously dimensioned when obtaining the optimal control. An advantage of this approach is that it might give shorter computation time because a loop over battery sizes is not needed.

III. Convex Optimization

Here, we give a brief background on convex optimization and discuss how convex optimization can be used to find a lower bound to the solution of the mixed-integer optimization problem.

A. Definition for a Convex Problem

A convex problem, in its general form, can be written as

$$\begin{aligned} \text{minimize} \quad & f_0(x) \\ \text{subject to} \quad & f_i(x) \le 0, \quad i = 1, \ldots, m \\ & h_j(x) = 0, \quad j = 1, \ldots, p \\ & x \in \mathcal{X} \end{aligned}$$

where $\mathcal{X} \subseteq \mathbb{R}^n$ is a convex set, $f_i(x)$ are convex functions, and $h_j(x)$ are affine in the vector of decision variables $\boldsymbol{x}$ [16]. For the dimensioning problem (7), vector $\boldsymbol{x}$ will be very large (thousands of elements) because it will include the optimization variables in (7) for all the time instances $t_k \in \mathcal{T}$ of a typically large discrete set $\mathcal{T}$. Moreover, the problem (7) has only affine functions in equality constraints and nonlinear functions in inequality constraints [hence, the reason for relaxing (1) and (2)], but it is not convex. This is because, even when $\boldsymbol{n}$ is considered a real number, control variable $\boldsymbol{e}(t)$ belongs to an integer set. In addition, product $\boldsymbol{P}_g(t)\boldsymbol{e}(t)$ is not a convex function, even if $\boldsymbol{e}(t)$ could be relaxed to a real number.

B. Lower Bound to the Mixed-Integer Problem

A common approach to optimizing mixed-integer problems is to relax the integer variables to real value variables [21]. The obtained solution of the relaxed problem is then a lower bound to the mixed-integer problem. Moreover, if the optimal values of the relaxed variables are nearly integer, then techniques exist, which is not very computationally demanding, to obtain the optimal solution of the mixed-integer problem [21]. Here, we investigate whether or not the relaxation of the engine on/off control should be used for obtaining the optimal solution of the mixed integer, dimensioning, and control problem (7), when $\boldsymbol{n}$ is considered a real number.

With $\boldsymbol{e}(t)$ relaxed to a real value, a convex form of (7) can be obtained by introducing variable change $\tilde{\boldsymbol{P}}_g(t) = \boldsymbol{P}_g(t)\boldsymbol{e}(t)$. This will replace (3), (7c), (7e), and (7j) with

$$P_f\left(\tilde{\boldsymbol{P}}_{\boldsymbol{g}}(t), \boldsymbol{e}(t)\right) = a_0 \frac{\tilde{\boldsymbol{P}}_{\boldsymbol{g}}^{\boldsymbol{2}}(t)}{\boldsymbol{e}(t)} + a_1 \tilde{\boldsymbol{P}}_{\boldsymbol{g}}(t) + a_2 \boldsymbol{e}(t) \tag{8a}$$

$$\begin{aligned} \boldsymbol{T}(t)\omega(t) + P_{\text{loss}}\left(\boldsymbol{T}(t), t\right) \le P_b\left(\boldsymbol{i}(t), \boldsymbol{n}\right) \\ + \tilde{\boldsymbol{P}}_{\boldsymbol{g}}(t) + \boldsymbol{P}_c(t)c(t) - P_a \end{aligned} \tag{8b}$$

$$\tilde{\boldsymbol{P}}_{\boldsymbol{g}}(t) \in [0, \boldsymbol{e}(t)P_{g,\max}] \tag{8c}$$

$$\boldsymbol{e}(t) \in (0, 1] \tag{8d}$$

where $\boldsymbol{e}(t)$ is limited to strictly positive to avoid division by zero in (8a).

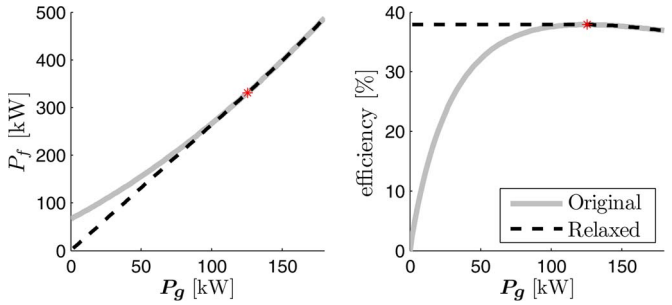

Fig. 4. Original and relaxed EGU models. For generator power lower than the power at peak efficiency, the efficiency of the relaxed model is equal to the peak efficiency of the original model. Above this point, the efficiency of the relaxed model follows the efficiency of the original model.

This convex problem can be easily solved with publicly available tools, e.g., SeDuMi [22], but the implications from the relaxation of $\boldsymbol{e}(t)$ can also be reasoned analytically. It can be easily found that the optimal value $\boldsymbol{e}^*(t)$ that minimizes the fuel power (8a) can be expressed as a function of the generator power, i.e.,

$$\boldsymbol{e}^*(t) = \min\left\{\tilde{\boldsymbol{P}}_{\boldsymbol{g}}(t)\sqrt{a_0/a_2}, 1\right\}.$$

When this is replaced back to (8a), an expression can be obtained

$$P_f^*\left(\tilde{\boldsymbol{P}}_{\boldsymbol{g}}(t)\right)=\begin{cases}\tilde{\boldsymbol{P}}_{\boldsymbol{g}}(t)\left(2\sqrt{a_0a_2}+a_1\right), & \tilde{\boldsymbol{P}}_{\boldsymbol{g}}(t)\le\sqrt{a_2/a_0}\\ a_0\tilde{\boldsymbol{P}}_{\boldsymbol{g}}^{\boldsymbol{2}}(t)+a_1\tilde{\boldsymbol{P}}_{\boldsymbol{g}}(t)+a_2, & \text{otherwise}\end{cases}$$

which indicates that the relaxation of $\boldsymbol{e}(t)$ causes significant changes to the original EGU model, as shown in Fig. 4. Namely, the relaxed EGU model removes an important limitation of the ICE, i.e., the low efficiency during idling. Without this limitation, the optimal control $\boldsymbol{e}^*(t)$ is not mainly binary but a continuous value in (0, 1] that smoothly follows the changes in demanded power. Hence, besides using it as a lower bound, the solution of this relaxed problem will not be used for obtaining the solution of the mixed-integer problem.

IV. Heuristics Based on Costate

Here, we introduce a novel strategy for optimal control of the studied mixed-integer problem. The strategy starts by deciding feasible values for the integer variable $\boldsymbol{e}(t)$ at each point of time. Then, the optimization problem (7) becomes a convex subproblem that can be solved to obtain the optimal values of the rest of the optimization variables. The optimal solution of the subproblem is used to improve iteratively the initial choice of $\boldsymbol{e}(t)$ in the direction of minimizing the optimization cost of the convex subproblem solved in a loop. A method to obtain an initial feasible solution for $\boldsymbol{e}(t)$ is discussed later in Section IV-B.

At the optimal solution of the subproblem, the Hamiltonian [18], [19] is investigated as follows:

$$\mathcal{H}^*(\cdot) = J\left(\boldsymbol{P}_{\boldsymbol{g}}^*(t), \boldsymbol{P}_{\boldsymbol{c}}^*(t), \boldsymbol{e}(t)\right) - V\boldsymbol{\lambda}^*(t)\boldsymbol{i}^*(t) \qquad (9)$$

which gives an equivalent fuel–electricity cost at each time instance on the bus line. The symbol $\cdot$ in $\mathcal{H}^*(\cdot)$ represents a compact notation of a function of decision variables, and $\lambda(t)$ is the costate of the system, which is also known as the adjoint state or the Lagrange multiplier [23], [24]. In the optimal control of hybrid vehicles, $-\lambda(t)$ is also referred to as the equivalence factor [25], [26] since it translates the electric energy used by the EM to an equivalent fuel consumption. In this paper, the unit of $\lambda(t)$ is in currency/kWh.

A. Costate Heuristic Method

The idea of the costate method is built upon the assumption that the optimal costate of the convex subproblem is close to the globally optimal costate of the mixed-integer problem. First an initial feasible value for $\boldsymbol{e}(t)$ is decided, the convex subproblem is solved, and the costate $\boldsymbol{\lambda}^*(t)$ is obtained. Then, this costate is used to modify the initial integer control $\boldsymbol{e}(t)$, which when used again in the convex subproblem may further decrease the cost.

To decide at which time instances $\boldsymbol{e}(t)$ is to be modified, a so-called complementary Hamiltonian is constructed $\tilde{\mathcal{H}}(\neg\boldsymbol{e}(t),\cdot)$, where the engine on/off signal has a flipped value at each time instance (here, $\boldsymbol{e}(t)$ is also used as a Boolean variable). In this context, $\tilde{\mathcal{H}}(\neg\boldsymbol{e}(t),\cdot)$ is a measure of the possible decrease in cost by changing the integer control $\boldsymbol{e}(t)$ at certain time instances. At a predefined number N_f of time instances with the highest difference $\mathcal{H}^*(\boldsymbol{e}(t),\cdot) - \tilde{\mathcal{H}}^*(\neg\boldsymbol{e}(t),\cdot)$, the value of $\boldsymbol{e}(t)$ is flipped, and the convex subproblem is solved again for the recently obtained $\boldsymbol{e}(t)$. This procedure is repeated while there are improvements in the cost, and it can be summarized as follows.

1) A feasible solution for the integer control $\boldsymbol{e}(t)$ is decided, and the globally minimal cost is assigned infinity, such that the first feasible solution will be accepted.
2) For the choice of $\boldsymbol{e}(t)$, the optimal solution of the convex subproblem is obtained. If the problem is infeasible or there is no improvement in cost, then go to step 5.
3) From the solution of the subproblem, the optimal costate $\boldsymbol{\lambda}^*(t)$ is obtained. Using the costate, $\mathcal{H}^*(\boldsymbol{e}(t),\cdot)$ is computed, and $\tilde{\mathcal{H}}(-\boldsymbol{e}(t),\cdot)$ is minimized.
4) The value of $\boldsymbol{e}(t)$ is flipped at N_f time instances with the highest difference $\mathcal{H}^*(\boldsymbol{e}(t),\cdot) - \tilde{\mathcal{H}}^*(-\boldsymbol{e}(t),\cdot)$, and the algorithm goes back to step 2.
5) If $N_f > 1$, then $N_f = \text{round}(N_f/2)$; the last change of $\boldsymbol{e}(t)$ is canceled, and the algorithm goes back to 4. Exit otherwise.

The initial value for $N_f = N_{\text{init}}$ is an engineering decision that may affect the number of iterations needed by the algorithm. If the initial solution is known to be close to the global optimum, then N_{init} can be chosen to be rather small. If the initial solution is known to be far from the global optimum or if there is no knowledge about it, then N_{init} can be as large as 50% of the number of time samples in the bus line. However, choosing a large value for N_{init} will not significantly degrade the performance of the algorithm. In a worst-case scenario where N_{init} is large and the initial engine on/off control differs from the global optimum in only one time instance, the algorithm will need to solve the convex subproblem

$\log_2 N_{\text{init}}$ times before N_f decreases to 1 and before a change in $\boldsymbol{e}(t)$ is eventually performed.

Later, in the examples in Section V, the initial value for N_f has been chosen to be half the number of time samples in the bus line.

B. Feasible Engine On/Off Control

If the mixed-integer problem (7) has a feasible solution, then a trivial solution is choosing $\boldsymbol{e}(t)$ that never turns off the engine. A better solution is to turn on the engine only for high power demands where the EGU is more efficient. Such a solution has been proposed in [15], where the engine is turned on when the power $P_{\text{base}}(t)$ of the vehicle without the weight of the battery exceeds a certain threshold P^*_{on}.

Assuming that, within the slide-in interval, the vehicle will be mainly driven by grid power, a feasible on/off control is

$$\boldsymbol{e}(t) = \begin{cases} 1, & P_{\text{base}}(t) - \eta P_{c,\max} c(t) > P^*_{\text{on}} \\ 0, & \text{otherwise.} \end{cases} \tag{10}$$

The optimal power threshold P^*_{on} is different for different bus lines. For each bus line, P^*_{on} can be found as the threshold that gives a feasible solution and minimizes the cost of the convex subproblem iteratively solved for several gridded (discrete) values $P_{\text{on}_j} \in [0, P_{g,\max}]$ within the power range of the vehicle.

Note that, with this procedure, the optimal battery size and powertrain control can be obtained simultaneously. This is because, for a given $\boldsymbol{e}(t)$, the optimization subproblem (7) is convex in $\boldsymbol{n}$ and in the optimization variables $\boldsymbol{P}_g(t), \boldsymbol{P}_c(t), \boldsymbol{T}(t), \boldsymbol{E}(t)$ and $\boldsymbol{i}(t)$. Moreover, it has been shown in [15] that this solution is close to the global optimum, both in total optimization cost and battery size. This is also observed in the results in Section V-D.

C. Computing the Costate

Most solvers of convex problems, e.g., SeDuMi [22], provide the Lagrangian dual variables together with the primal optimal solution. Then, the costate required in (9) will be the dual variable associated to constraint (7g). Here, however, the costate will be derived from the Pontryagin's maximum principle [17]. This gives a better insight on the nature of the costate function and on the time instances at which the costate is not strictly defined. For didactic reasons, the process is described through a snapshot (see Fig. 5) taken during the iterations of the costate algorithm for an example of optimal battery dimensioning and control of a PHEV bus. The snapshot depicts the optimal SOC and the costate trajectory of the convex subproblem of the bus driven on the bus line shown in Fig. 2, with a battery consisting of 10-Ah cells.

1) Necessary Conditions: The necessary condition for an extremum of the Hamiltonian

$$\frac{d\boldsymbol{\lambda}^*(t)}{dt} = -\left(\frac{\partial \mathcal{H}(\cdot)}{\partial \boldsymbol{E}(t)}\right)^* = 0 \quad \forall t \in \mathcal{T}_E \tag{11}$$

reveals that the costate is constant in time intervals $\mathcal{T}_E$ without active state constraints since $\mathcal{H}(\cdot)$ does not explicitly depend on $\boldsymbol{E}(t)$. By introducing operator free$(\boldsymbol{E}(t))$ that gives "true" if (7h) is not active, set $\mathcal{T}_E$ can be mathematically described by

$$\mathcal{T}_E = \{t \in [t_0, t_f] \mid \text{free}\,(\boldsymbol{E}(t))\}\,. \tag{12}$$

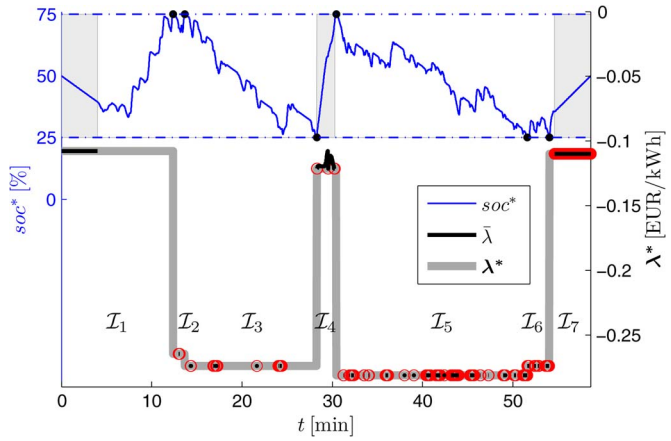

Fig. 5. Battery SOC on the left axis and the costate on the right axis. The costate is a piecewise constant function where the different pieces belong to the time intervals $\mathcal{I}_k, k = 1, \ldots, 7$. The time instances where the value of the costate can be obtained from (14) are represented by circles. Charging opportunities are depicted by shaded regions.

The value of the costate in these intervals can be obtained from the second necessary condition for an extremum, i.e.,

$$\left(\frac{\partial \mathcal{H}(\cdot)}{\partial \boldsymbol{u}(t)}\right)^* = 0 \quad \forall t \in \{\mathcal{T}_1 \cup \mathcal{T}_2\} \tag{13}$$

with $\boldsymbol{u}(t) = [\boldsymbol{i}(t) \quad \boldsymbol{P}_c(t) \quad \boldsymbol{P}_g(t) \quad \boldsymbol{T}(t)]^T$, at time instances $t \in \{\mathcal{T}_1 \cup \mathcal{T}_2\}$ without active constraints on control signals of $\boldsymbol{u}^*(t)$. Moreover, the convexity of the problem ensures that $\mathcal{H}^*(\cdot)$ is in fact a minumum, i.e.,

$$\frac{\partial^2 \mathcal{H}(\cdot)}{\partial \boldsymbol{u}^2}(t) \geq 0 \quad \forall t \in [t_0, t_f].$$

For a chosen on/off control $\boldsymbol{e}(t)$, the convex optimization will find $\boldsymbol{u}^*(t)$ that minimizes the total cost of the subproblem, and the only unknown in (13) will be $\boldsymbol{\lambda}^*(t)$. It can be shown (see Appendix B) that the optimal costate, which is denoted by circles in Fig. 5, is

$$\boldsymbol{\lambda}^*(t) = \begin{cases} -w_f \left(2a_o \boldsymbol{P}^*_{\boldsymbol{g}}(t) + a_1\right)\left(1 - \frac{2R}{\boldsymbol{n}^* V}\boldsymbol{i}^*(t)\right), & t \in \mathcal{T}_1 \\ -\frac{w_c}{\eta}\left(1 - \frac{2R}{\boldsymbol{n}^* V}\boldsymbol{i}^*(t)\right), & t \in \mathcal{T}_2 \end{cases} \tag{14}$$

with the sets $\mathcal{T}_1$ and $\mathcal{T}_2$ described by

$$\mathcal{T}_1 = \left\{t \in [t_0, t_f] \mid \boldsymbol{e}(t) \wedge \neg c(t) \wedge \text{free}\,(\boldsymbol{i}^*(t)) \wedge \text{free}\left(\boldsymbol{P}^*_{\boldsymbol{g}}(t)\right)\right\}$$

$$\mathcal{T}_2 = \{t \in [t_0, t_f] \mid \text{free}\,(\boldsymbol{i}^*(t)) \wedge \text{free}\,(\boldsymbol{P}^*_{\boldsymbol{c}}(t)) \wedge c(t) \wedge \left(\boldsymbol{e}(t) \wedge \text{free}\left(\boldsymbol{P}^*_{\boldsymbol{g}}(t)\right) \vee \neg \boldsymbol{e}(t)\right)\}$$

where free$(\boldsymbol{i}(t))$, free$(\boldsymbol{P}_g(t))$, and free$(\boldsymbol{P}_c(t))$ give true if the constraints (7d)–(7f), respectively, are not active.

Because $\boldsymbol{\lambda}^*(t)$ is a piecewise constant function, it can be completely reconstructed along the bus line if each of the intervals $\mathcal{I}_k$ contains at least one time instance $t \in \{\mathcal{T}_1 \cup \mathcal{T}_2\}$.

Note that (13) may hold with equality at other time instances not belonging to $\mathcal{T}_1$ and $\mathcal{T}_2$, when $\boldsymbol{u}^*(t)$ is inside the bounded region and the optimal solution is singular. However, the singularity of the solution will not be explicitly studied. Instead, to obtain more information on the costate, its upper bound will be investigated.

2) Upper Bound to the Costate: When no time instance in $\mathcal{I}_k$ belongs to $\mathcal{T}_1$ or $\mathcal{T}_2$, the value of the costate in $\mathcal{I}_k$ cannot be obtained from (14). Such a situation is depicted in $\mathcal{I}_1$ in Fig. 5, where it was found optimal to not charge from the grid during the first charging opportunity. (With the high power battery cells, the vehicle can recuperate the free-of-charge braking energy available at the beginning of the cycle due to the negative road gradient.)

In these cases, the costate is assigned an upper bound $\bar{\boldsymbol{\lambda}}(t)$, i.e.,

$$\boldsymbol{\lambda}^*(t) = \min \mathcal{L}_k \quad \forall t \in \mathcal{I}_k$$
$$\mathcal{L}_k = \left\{\bar{\boldsymbol{\lambda}}(t) \mid t \in \mathcal{I}_k\right\}$$

with $\bar{\boldsymbol{\lambda}}(t)$ being computed exactly as in (14) but with $\mathcal{T}_1$ and $\mathcal{T}_2$ replaced by

$$\mathcal{T}_3 = \{t \in [t_0, t_f] \mid \boldsymbol{e}(t) \wedge \neg c(t)\}$$
$$\mathcal{T}_4 = \{t \in [t_0, t_f] \mid c(t)\}$$

respectively. The upper bound $\bar{\boldsymbol{\lambda}}(t)$ can be interpreted as the value of the costate that will minimize the Hamiltonian in $\mathcal{I}_k$ with control $\boldsymbol{u}^*(t)$ that is free but very close to the bounds. (If $\bar{\boldsymbol{\lambda}}(t)$ is indeed the optimal costate in some time interval, i.e., $\bar{\boldsymbol{\lambda}}(t) = \boldsymbol{\lambda}^*(t)$, then the interval is a singular arc [27]).

Note that, although $\boldsymbol{\lambda}^*(t)$ is constant in $\mathcal{I}_k$, $\bar{\boldsymbol{\lambda}}(t)$ may not be constant (see, e.g., $\mathcal{I}_4$ in Fig. 5).

3) Intervals With the Undefined Costate: In time intervals $\mathcal{I}_k$ where no time instance belongs to $\bigcup_{j=1}^{4} \mathcal{T}_j$, neither the costate nor its upper bound can be computed. Experiments showed that such intervals are rare. Nevertheless, these intervals have been given the highest priority in the list of time instances where $\boldsymbol{e}(t)$ will be flipped. This action can be seen as a deliberate disturbance of $\boldsymbol{e}(t)$ that may give more constructive information on the succeeding iteration of the costate heuristic algorithm, i.e., in the succeeding iteration, some of these time instances may belong to $\bigcup_{j=1}^{4} \mathcal{T}_j$.

The set of all time instances where the costate is undefined is denoted by $\mathcal{T}_u$.

D. Complementary Hamiltonian

The complementary Hamiltonian $\tilde{\mathcal{H}}(\neg \boldsymbol{e}(t), \cdot)$ involved in step 4 of the costate algorithm is used to give an indication of what can be gained by flipping the value of the integer control $\boldsymbol{e}(t)$. When minimizing $\tilde{\mathcal{H}}(\neg \boldsymbol{e}(t), \cdot)$, the electric energy equivalence to fuel consumption, i.e., the costate $\boldsymbol{\lambda}^*(t)$, is considered to be equal to the one that minimizes the Hamiltonian $\mathcal{H}(\boldsymbol{e}(t), \cdot)$. Moreover, for the problem of simultaneous dimensioning and control, it is also assumed that the battery size $\boldsymbol{n}^*$ will stay equal to the one used in $\mathcal{H}^*(\boldsymbol{e}(t), \cdot)$. (This is further discussed in Section IV-B.) Thus, the optimization problem that minimizes the complementary Hamiltonian can be formulated as a convex problem, i.e.,

$$\text{minimize} \int_{\mathcal{T}_5} \left(J\left(\boldsymbol{P}_g(t), \boldsymbol{P}_c(t), \neg \boldsymbol{e}(t)\right) - \boldsymbol{\lambda}^*(t) V \boldsymbol{i}(t)\right) dt \quad (15a)$$

$$\text{subject to (7b)–(7f)}, \forall t \in \mathcal{T}_5 \quad (15b)$$

with optimization variables $\boldsymbol{P}_g(t)$, $\boldsymbol{P}_c(t)$, and $\boldsymbol{i}(t)$. Set $\mathcal{T}_5$ includes the time instances where $\boldsymbol{\lambda}^*(t)$ is obtained and where the battery and EGU can meet the power demand, i.e.,

$$\mathcal{T}_5 = \{t \in [t_0, t_f] \backslash \mathcal{T}_u \mid T_v(\boldsymbol{n}^*, t)\omega(t) + P_a + P_{\text{loss}}\left(T_v(\boldsymbol{n}^*, t), t\right) \leq P_{b,\max} + P_{g,\max} - \boldsymbol{e}(t) + \eta P_{c,\max} c(t)\}$$

with the maximum battery power found as

$$P_{b,\max} = \boldsymbol{n}^* \min\left\{V i_{c,\max} - R i_{c,\max}^2, \frac{V^2}{4R}\right\}.$$

At time instances $t \notin \mathcal{T}_5$, $\tilde{\mathcal{H}}^*(\cdot)$ has been assigned an infinite cost, making these time instances the least-desirable choices for flipping the engine on/off control as they will lead to infeasible solution.

E. Mixed-Integer Control Problems With Design Parameters

When minimizing the complementary Hamiltonian in (15), the battery size $\boldsymbol{n}^*$ is kept equal to the one used in $\mathcal{H}^*(\boldsymbol{e}(t), \cdot)$. The reason for doing this is to obtain a control problem without design parameters that could be easily analyzed using the classical optimal control theory [27]. A more detailed investigation of how to include the design parameter $\boldsymbol{n}$ when obtaining the extremum of $\tilde{\mathcal{H}}(\cdot)$ will be carried on in future studies. This will be particularly relevant if additional powertrain components, such as EMs, EGUs, and ICEs, are to be dimensioned simultaneously.

As a consequence, it can be expected that the complementary Hamiltonian may give indications on how to improve the initial integer control, but it may not give indications on how to improve the initial battery size in two consecutive iterations of the proposed algorithm. For this reason, the initial battery size of the simultaneous dimensioning and control subproblem (7) should be chosen close to the globally optimal battery size. A strategy for obtaining such an initial solution for the studied problem has been given in Section IV-B, and it is further verified in the example in Section V-D. However, for a general parameter design and control problem, it may not be easy to find such a solution. In that case, the proposed costate method could be used by iteratively solving the control problem for several fixed values of the design parameters.

V. Examples of Optimal Control and Battery Dimensioning

Here, we give several examples of optimal battery dimensioning and control of a PHEV bus. To obtain solutions (and lower bounds) to these examples, the following optimization methods/setups have been implemented.

- DP is used for obtaining the global optimum of the mixed-integer problem (7) for several fixed battery sizes. The solution from DP is used only for validation purposes. Details concerning its implementation are given in Appendix C.
- The proposed costate heuristic method is used for obtaining the optimal mixed-integer control for battery sizes that were also used in DP. In each step of the algorithm, the Hamiltonian is minimized, solving the convex optimal control subproblem (7) with both $\boldsymbol{e}(t)$ and $\boldsymbol{n}$ having fixed values. In the rest of this paper, this convex subproblem will be referred to as CF (Convex, Fixed battery).
- The proposed costate heuristic method is also used for solving the problem of simultaneous dimensioning and control. In each iteration of the algorithm, the convex subproblem (7) is solved, where $\boldsymbol{e}(t)$ is fixed, and $\boldsymbol{n}$ is a real-valued optimization variable. This convex subproblem will be referred to as CS (Convex, Sizing battery).
- The given two instances of the costate heuristic method include minimization of the complementary Hamiltonian. The convex problem (15) minimizing the complementary Hamiltonian will be referred to as CH.
- The lower bound to the mixed-integer problem is obtained by solving the convex problem described in Section III-B. The results are given in the last row of Table I, but they are not discussed further in this paper.

A. Problem Setup

The studied PHEV is equipped with a 220-kW EM and a 180-kW EGU, as in Fig. 4. Its battery can be either energy optimized with cell capacity of 44 Ah and a cost of 500 EUR/kWh, or power optimized with cell capacity of 10 Ah and cost of 1500 EUR/kWh. The allowed SOC range is within 25%–75%, and the operation is charge sustaining, where it is required to start and end at 50% SOC.

The battery sizing is investigated on four bus lines, from which the first bus line (L1) is given in Fig. 2, and the other three are certified emission test cycles available online.[1] The second bus line (L2) is the City Suburban Cycle, the third bus line (L3) is the Orange County Bus Cycle, and the fourth bus line (L4) is the Manhattan Bus Cycle repeated four times. On all four bus lines, the vehicle can charge for 4 min at each end and for 2 min 2 min while sliding in a tramline at about the middle of the bus line. The chargers have maximum power of 100 kW.

[1] The test cycles can be found on http://www.dieselnet.com/standards/cycles, March 2012.

B. Global Optimum

The global optimum obtained by DP is given in the first row of Table I, whereas the cost versus number of battery cells is shown in Fig. 6 and magnified around the optimum in Fig. 7. To make the comparison easier, the cost is given in Euros per 100 kilometers. The results indicate that both the battery type and the bus line have significant impact on the optimal battery size. The power limit of the chargers, however, does not affect the battery size as the vehicle never charges with rate greater than 63%. This is because battery losses increase with charging power, and second, the batteries are too expensive to be large enough to accumulate the available grid energy. In the case of the 44-Ah cells, it is the power limit of the cell that decides the battery size since these cells never reach high SOC [see Fig. 8(a)]. The battery with the 10-Ah cells is instead sized by its energy limit [see Fig. 8(b)].

The dimensioning problem is solved by running DP at gridded values of the battery size, where the grid is made denser around the global optimum. Within the magnified regions shown in Fig. 7, there are in total 176 battery sizes for all four bus lines and the two battery types (see the dot marker). The high number of investigated battery sizes is needed to improve the solution accuracy because, near the optimum, the cost may not vary much with battery size, and a difference of 100 battery cells may give just 1% change in total cost (see Fig. 6). For each fixed battery size, the algorithm requires about 1.5–2.5 h on a standard PC (2.67-GHz dual core CPU and 4-GB RAM), when configured for a highly accurate result. Hence, to keep the computation time within reasonable limits, the problem is solved using a computer cluster.

C. Results From the Costate Method

To investigate the performance of the costate method on the mixed-integer optimal control problem, CF is solved at the 176 fixed battery sizes that were also used in DP. Moreover, to better test the convergence of the costate method, the trivial initial solution is used, which keeps the engine on at all time instances.

The results are shown in Fig. 7 and show that the global optimum of the mixed-integer control problem (for fixed battery sizes) is reached for all the 176 battery sizes. More specifically, it was found that the distance to the global optimum (represented as relative error in total cost), i.e.,

$$\delta = \frac{\text{cost}_{\text{costate\_method}} - \text{cost}_{\text{DP}}}{\text{cost}_{\text{DP}}}$$

is below 0.03% for all the investigated cases. For more than 90% of the cases, the costate method gives even better result than DP (negative values in Table I). This is possibly due to the discretization error in DP or the error due to variable scaling in CF. Detailed results for the optimal battery sizes obtained by the costate method are shown in the second row in Table I.

One execution of CF requires about 4–10 s, whereas one execution of CH needs about 4–10 s, depending on the bus line. The costate method requires, on average, 20 executions of CF and 10 executions of CH. Hence, the optimal control for a fixed battery can be obtained in less than 5 min.

TABLE I
RESULTS FROM OPTIMIZATION WITH DP AND CONVEX OPTIMIZATION

Battery cell capacity		44 Ah				10 Ah				
Bus line		L1	L2	L3	L4	L1	L2	L3	L4	
Dynamic Programming (DP) for fixed battery sizes.	$\boldsymbol{n}$	157	92	237	296	138	121	174	168	
	J_{total}	45.75	39.22	46.37	52.78	30.85	23.60	24.42	31.04	EUR/100km
	J_{fuel}	29.85	27.24	20.24	22.46	20.72	11.53	8.39	16.57	EUR/100km
	J_{el}	4.04	5.03	8.22	7.95	2.79	5.62	6.78	5.53	EUR/100km
	J_{bat}	11.86	6.95	17.91	22.36	7.34	6.44	9.26	8.94	EUR/100km
	c_{rate}	36.48	24.53	49.14	62.14	9.41	21.53	29.58	29.52	%
Costate heuristic method for fixed battery sizes. The convex sub-problem used in the method is CF.	$\boldsymbol{n}$	157	92	237	296	138	121	174	168	
	J_{total}	45.75	39.21	46.37	52.76	30.85	23.60	24.42	31.03	EUR/100km
	J_{fuel}	29.84	27.22	20.24	22.43	20.72	11.53	8.38	16.57	EUR/100km
	J_{el}	4.05	5.04	8.22	7.97	2.79	5.62	6.78	5.53	EUR/100km
	J_{bat}	11.86	6.95	17.91	22.36	7.34	6.44	9.26	8.94	EUR/100km
	δ	0.01	-0.02	-0.00	-0.03	0.01	-0.00	-0.03	-0.01	%
Costate heuristic method for simultaneous dimensioning and control. The convex sub-problem used in the method is CS.	$\boldsymbol{n}$	156.93	78.11	254.96	304.97	137.93	121.53	174.90	168.13	
	J_{total}	45.76	39.30	46.52	52.84	30.84	23.60	24.42	31.03	EUR/100km
	J_{fuel}	29.86	28.71	18.81	21.63	20.72	11.49	8.31	16.56	EUR/100km
	J_{el}	4.05	4.69	8.45	8.17	2.79	5.64	6.80	5.53	EUR/100km
	J_{bat}	11.86	5.90	19.26	23.04	7.34	6.47	9.31	8.95	EUR/100km
	δ	0.02	0.20	0.32	0.12	-0.02	-0.00	-0.03	-0.01	%
Initial solution for the costate method using CS. The initial engine on/off control is found by (10).	$\boldsymbol{n}$	158.14	78.43	254.96	313.25	137.93	121.53	184.73	168.13	
	J_{total}	45.77	39.36	46.54	53.08	31.11	23.61	24.46	31.04	EUR/100km
	J_{fuel}	29.75	28.74	18.82	21.06	20.98	11.51	7.65	16.57	EUR/100km
	J_{el}	4.07	4.70	8.45	8.35	2.79	5.64	6.98	5.53	EUR/100km
	J_{bat}	11.95	5.93	19.26	23.67	7.34	6.47	9.83	8.95	EUR/100km
	δ	0.05	0.37	0.37	0.57	0.85	0.07	0.15	0.02	%
Lower bound to the dimensioning problem.	$\boldsymbol{n}$	66.28	4.52	108.20	245.22	137.93	117.72	170.40	168.13	
	J_{total}	40.69	33.37	39.98	50.00	30.58	23.33	24.24	30.82	EUR/100km

J_{total}, J_{fuel}, J_{el} and J_{bat} are the total optimization cost, fuel cost, cost for used electricity, and cost for battery, respectively; δ is relative error in total cost; c_{rate} is average charging rate from the chargers at the ends of the bus line.

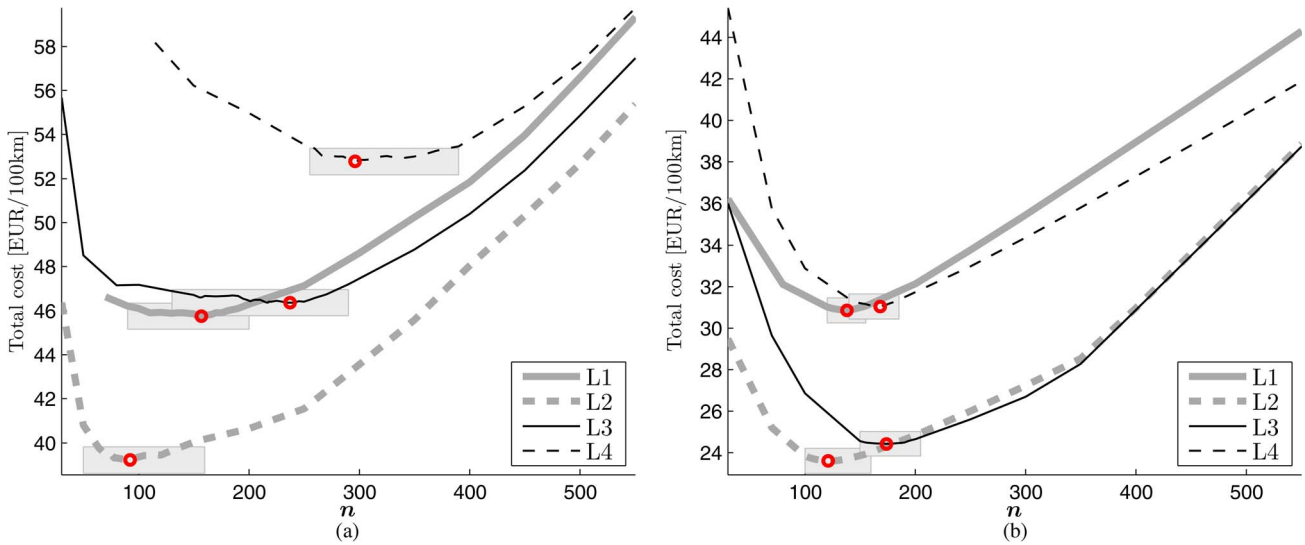

Fig. 6. Optimal cost versus battery size obtained by DP. The circles indicate the global optimum of the battery dimensioning problem. The shaded regions around the optimum are magnified in Fig. 7. (a) Battery cell capacity is 44 Ah. (b) Battery cell capacity is 10 Ah.

D. Simultaneous Dimensioning and Control

Here, the costate method is used to solve the problem of simultaneous dimensioning and control when the battery size is a real-valued optimization variable. The purpose of this example is to show that the proposed costate method may not perform well on the control problem with design parameters.

First, an initial solution is chosen with the engine turned on at all time instances. The investigated PHEV is driven on L3 using the energy optimized battery cells, and the successive steps of the costate algorithm are shown in Fig. 9(a).

This example shows that the costate method is not able to move the battery size further from the initial value. There are two reasons for this: One is that, at this stage of development, no mechanism has been implemented to improve the battery size when minimizing the complementary Hamiltonian, as discussed in Section IV-D. The other reason is a premature convergence that traps the solution in a local minimum. With

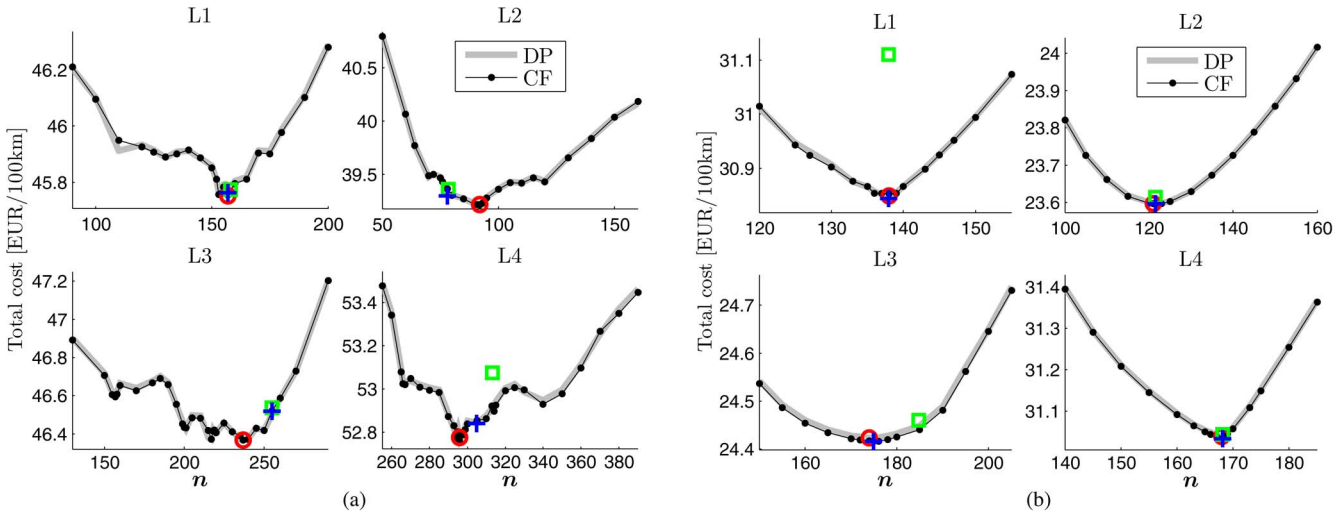

Fig. 7. Optimal cost versus battery size. The solution of the mixed-integer control problem solved by DP for fixed battery sizes is indicated by the thick line, whereas the global optimum of the dimensioning problem is depicted by the circle. The optimal solution of the costate method (using CF) for the mixed-integer control problem is found at the fixed battery sizes indicated by the dot marker. The solution of the costate method (using CS) for simultaneous dimensioning and control is indicated by the plus. The initial solution of the latter costate method, where the initial engine on/off control is obtained from (10), is indicated by the square. (a) Battery cell capacity is 44 Ah. (b) Battery cell capacity is 10 Ah.

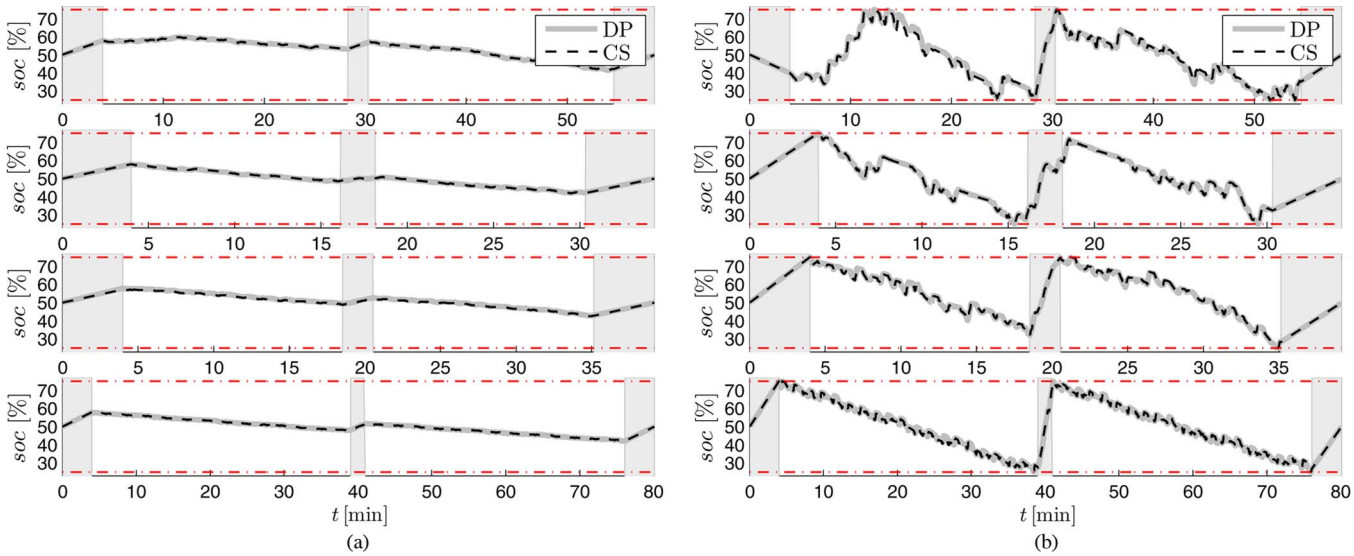

Fig. 8. Optimal battery SOC trajectories obtained by DP and convex optimization of the simultaneous sizing and control subproblem (CS) using costate heuristics for the engine on/off control. The four plots, from top to bottom, represent the four bus lines L1–L4. Charging opportunities are depicted by the shaded regions. (a) Battery cell capacity is 44 Ah. (b) Battery cell capacity is 10 Ah.

the engine on at all time instances, CS gives small battery size. Then, for this battery size, the complementary Hamiltonian suggests many (N_f) time instances at which the engine on/off control flips value, thus drastically decreasing the total cost. In the succeeding step, when the Hamiltonian is minimized for the recently obtained on/off control, the solution is already trapped in a local minimum, and CS gives a battery size that is close to the initial battery size. In certain cases, the algorithm may still converge to the global optimum, as shown in the example in Fig. 9(b). However, a general conclusion can be drawn that the costate method may decrease the initial cost by improving the engine on/off control, but it may not be able to improve the design parameter; therefore, it may be crucial to start with an initial battery size that is close to the optimal battery size.

Second, the costate method is evaluated with a better initial solution where the initial engine on/off control is obtained from (10). It can be noticed in the fourth row in Table I that this initial solution is already within 0.9% to the global optimum, thus supporting the same outcome observed in [15] that even this simple heuristic choice is a viable approach when dimensioning PHEVs with a series topology. Starting from this feasible solution, the costate method further decreases the difference in total cost to less than 0.35%, which has been shown in the third row of Table I.

The optimal SOC trajectories of both DP and the costate method are shown in Fig. 8. It can be seen that both algorithms point to the same solution as the lines almost completely overlap.

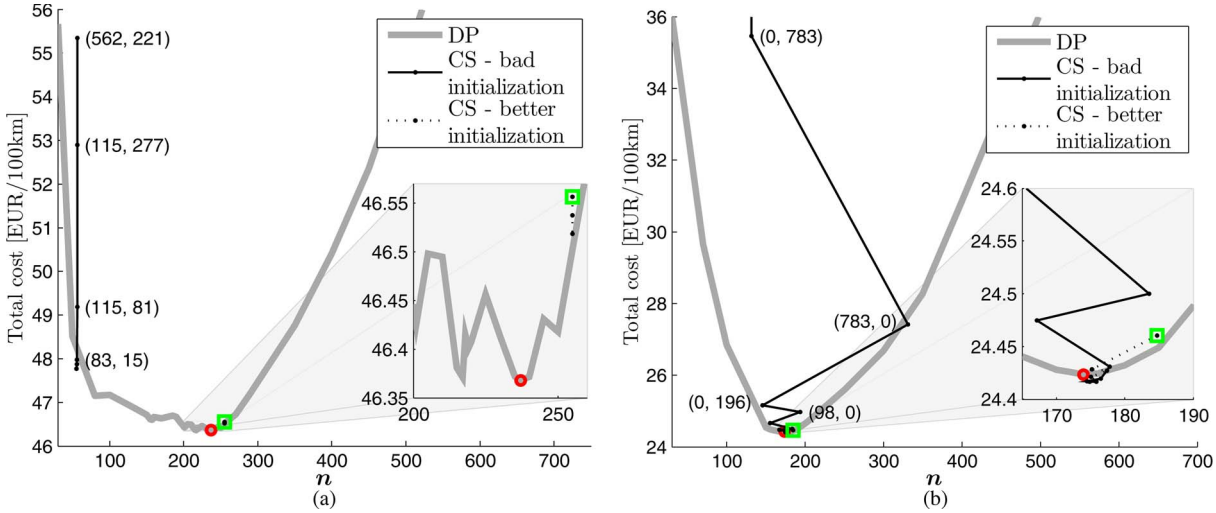

Fig. 9. Successive steps of the costate method for simultaneous dimensioning and control of the PHEV driven on L3. The direction of movement is toward decreasing the total cost. The thin solid and dotted lines show evaluations of the algorithm with the initial solution $\mathbf{e}(t) = 1 \forall t \in [t_0, t_f]$ and with the initial solution obtained from (10), respectively. The latter (better) initial solution is indicated by a square. The boxed shaded regions to the right of the plots are magnifications around the global optimum indicated by a circle. The first number and the second number in parentheses show the number of time instances the engine is turned on and off, respectively, in the first few iterations of the algorithm. (a) Battery cell capacity is 44 Ah. (b) Battery cell capacity is 10 Ah.

The total computation time needed to solve the problem of simultaneous dimensioning and control is less than 16.3 min. Up to 10 min of this time are needed to obtain the initial solution. This is because 30 power levels are investigated to obtain the optimal power threshold above which the engine is turned on, and for each power level, CS is solved in about 8–20 s, depending on the bus line. The remaining 6.3 min are due to the costate method that requires executing CS and CH, 15 and eight times on average, respectively.

VI. Discussion and Future Work

Here, we point out the key benefits of the proposed methodology and discuss possibilities for further studies.

A. Multidimensional Problems

This paper showed an alternative approach to solving the 1-D (one state) battery sizing and control problem. The simplicity of the problem allowed it to be solved with DP. In this paper, DP was configured to deliver very high accuracy that may not be necessary in industrial applications. Moreover, dedicated solvers exist [28], which may further decrease the computation time of DP to be comparable with the costate method.

However, the true advantage of the proposed method is in the possibility of optimizing multidimensional problems for which DP will need very long computation time. One example could be simultaneous dimensioning and control of a powertrain with two or more energy buffers, as investigated in [15], or an optimal control of a powertrain with thermal states of the vehicle components, such as the battery, the EM, the EGU, the catalytic converter, and the passenger compartment. This is particularly important for the electric components that could easily overheat if not managed properly. (An example illustrating convex modeling steps for including a thermal state in the model is given in [29].)

Each new state in the multidimensional model will introduce an additional costate in the Hamiltonian. This will affect the costate method, and future work is needed to extend the method to such cases.

B. Future Studies

The examples in this paper showed that, using costate heuristics for the engine on/off control, the solution of the dimensioning problem (using CS) is close to the global optimum, whereas the control problem (CF) for a fixed battery size practically reaches the global optimum. Although experimental, these results are promising and certainly show the need for further studies to investigate in which cases the algorithm will converge and in which it may not.

The computation time required by the costate method is short, which is about 5 min for a fixed battery size, but it could be decreased even further. For example, instead of using CH that requires 4–10 s, $\tilde{\mathcal{H}}^*(\cdot)$ can be solved analytically in milliseconds. Similarly, $\mathcal{H}^*(\cdot)$ could also be analytically solved if it is known that the state is not activating any constraints, as with the 44-Ah cell. Then, the costate is constant, it needs to be computed only once, and it can be found either by convex optimization or by root finding algorithm that gives a costate, which preserves the charge-sustained operation [30].

Future studies may focus on extending the strategy on problems with more integer control variables, e.g., parallel powertrains that have gears as an additional integer control signal. If the set of discrete values for the integer variables is small, then the costate strategy can be immediately applied by constructing new complementary Hamiltonian for each new discrete value. If the discrete set is large, then instead of using complementary Hamiltonians, improved values for the integer variable could be obtained using solvers for integer problems or with DP. These solvers will need relatively short computation time because the costates can be used to eliminate the need for the continuous

states in the problem. (Of course, the same assumption will be used, i.e., the optimal costates will not change much between two consecutive iterations of the proposed algorithm.)

Investigations are also needed for problems where states are integer variables. For example, the PHEV transportation problem could be easily transformed into an integer state problem if the model penalizes (or prevents) frequent engine on/off switching. An example of such model can be found in [15].

VII. Conclusion

This paper has presented a method for optimal control of mixed-integer problems that, for given feasible values of the integer variables, are convex in the rest of the variables. The method allows the problem to be solved in relatively short time using convex optimization techniques while obtaining a solution near the global optimum.

The method has been applied on the problem of optimal battery dimensioning and control of a PHEV bus, where the only integer variable is the engine on/off control. The results showed that the problem can be solved in less than 17 min with less than 0.35% difference from the global optimum. Moreover, the results showed that the global optimum is practically reached (difference of less than 0.03%) for the optimal control problem of a PHEV with fixed battery.

Future studies may focus on adapting the method to problems with more integer control signals and design parameters.

Appendix A
Data for the Transportation Problem

Denoting the velocity and slope of the bus line by $v(t)$ and $\alpha(t)$, respectively, the angular velocity and torque demanded on the shaft between the EM and the differential can be computed as

$$\begin{aligned}\omega(t) &= \frac{\gamma}{r} v(t) \\ T_v(\boldsymbol{n}, t) &= \frac{gr}{\gamma} \left(m + \boldsymbol{n} m_{bc}\right) \left(c_r \cos \alpha(t) + \sin \alpha(t)\right) \\ &\quad + \frac{\rho A c_d r^3}{2\gamma^3} \omega^2(t) \\ &\quad + \left(I_{\mathrm{EM}} + \frac{I}{\gamma^2} + (m + \boldsymbol{n} m_{bc}) \frac{r^2}{\gamma^2}\right) \dot{\omega}(t)\end{aligned}$$

where g is the gravitational acceleration, ρ is the air density, and the rest of the parameters are described in Table II. The model neglects the inertial effects of the EGU.

Traction power to the wheels is delivered by a 220-kW EM, as in Fig. 10. (Losses of the power electronics are considered within the EM.)

The 10-Ah and 44-Ah cells have mass of 600 and 900 g, resistance of 0.9 and 2 mΩ, maximum charging current of 300 and 50 A, and maximum discharging current of 1000 and 50 A, respectively. The additional mass due to packaging and circuitry is 14.5%. The payment for both batteries is equally divided into $y = 2$ years with $p = 5\%$ yearly interest rate. By denoting with c_b the battery price in currency/kWh, the equivalent cell cost related to the driven bus line is obtained by multiplying the length of the bus line with the cell price per kilometer, given the average travel distance in one year, i.e., $d = 50\,000$ km. This yields

$$w_b = c_b E_s m_{bc} \left(1 + p \frac{y+1}{2}\right) \frac{\int_{t_0}^{t_f} v(t) dt}{yd}$$

where E_s [kWh/kg] is the specific energy of the entire energy content of the battery cell.

TABLE II
Parameter Values

Vehicle frontal area	$A = 7.54\,\mathrm{m}^2$
Aerodynamic drag coefficient	$c_d = 0.7$
Rolling resistance coefficient	$c_r = 0.007$
Wheel radius	$r = 0.509\,\mathrm{m}$
Final gear	$\gamma = 4.7$
Vehicle mass without the battery	$m = 14.5\,\mathrm{t}$
EM inertia	$I_{EM} = 2.3\,\mathrm{kgm}^2$
Inertia of final gear and wheels	$I = 41.8\,\mathrm{kgm}^2$
Charging stations efficiency	$\eta = 92\,\%$
Power used by auxiliaries	$P_a = 7\,\mathrm{kW}$
Fuel price	$w_f = 0.11\,\mathrm{EUR/kWh}$
Electricity price	$w_c = 0.1\,\mathrm{EUR/kWh}$
Sampling time	$1\,\mathrm{s}$

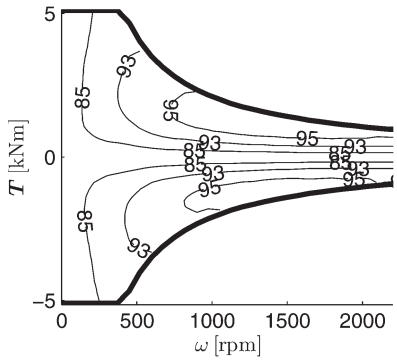

Fig. 10. Model of the EM. The thin lines represent efficiency, and the thick lines are the torque bounds.

Appendix B
Analytical Derivation of the Costate

To simplify the complex mathematical expressions in the following, the functions dependence on time will not be shown.

For a given battery size $\boldsymbol{n}^*$ that minimizes $\mathcal{H}$, the torque of the EM can be uniquely determined via

$$\boldsymbol{T}^* = \max\left\{\max\{T_{\min}, T_{b,\min}\}, T_v(\boldsymbol{n}^*)\right\}$$

where $T_{b,\min}$ is the equivalent torque limit in the EM imposed by the battery charging with the maximum current. It can be computed from (2) by considering zero EGU and grid power as follows:

$$T_{b,\min}\omega + P_{\mathrm{loss}}(T_{b,\min}) + P_a = P_{b,\min} = \left(V i_{c,\min} - R i_{c,\min}^2\right) \boldsymbol{n}^*.$$

The EGU power can also be described from (2) as follows:

$$\boldsymbol{P}_{\boldsymbol{g}}^* = \boldsymbol{T}^* \omega + P_{\mathrm{loss}}(\boldsymbol{T}^*) + P_a - P_b(\boldsymbol{i}^*, \boldsymbol{n}^*) - \boldsymbol{P}_{\boldsymbol{c}}^* \qquad (16)$$

leaving only two variables, i.e., $\boldsymbol{i}^*$ and $\boldsymbol{P}_c^*$, at which the extremum of $\mathcal{H}$ will be investigated. If these variables are free, then, at the extremum, it holds that

$$\left(\frac{\partial \mathcal{H}}{\partial \boldsymbol{i}}\right)^* = -w_f\left(2a_o\boldsymbol{P}_{\boldsymbol{g}}^* + a_1\right)\left(V - \frac{2R}{\boldsymbol{n}^*}\boldsymbol{i}^*\right) - \boldsymbol{\lambda}^* V = 0 \tag{17}$$

$$\left(\frac{\partial \mathcal{H}}{\partial \boldsymbol{P}_c}\right)^* = -w_f\left(2a_o\boldsymbol{P}_{\boldsymbol{g}}^* + a_1\right) + \frac{w_c}{\eta} = 0. \tag{18}$$

The costate can be computed at time instances covered by the following three cases.

1) If the engine is on, there is a charging opportunity, and the constraints (7d)–(7f) are not active (whether a constraint is active is decided with a tolerance of 0.01% of the expected signal's magnitude), the costate can be obtained by replacing P_g^* from (18) in (17), giving

$$\boldsymbol{\lambda}^* = -\frac{w_c}{\eta}\left(1 - \frac{2R}{\boldsymbol{n}^* V}\boldsymbol{i}^*\right). \tag{19}$$

2) If the engine is on, there is no charging opportunity, and the constraints (7d) and (7e) are not active; then, $\boldsymbol{P}_c^* = 0$, and the costate can be obtained from (17) as follows:

$$\boldsymbol{\lambda}^* = -w_f\left(2a_o\boldsymbol{P}_{\boldsymbol{g}}^* + a_1\right)\left(1 - \frac{2R}{\boldsymbol{n}^* V}\boldsymbol{i}^*\right).$$

3) If the engine is off, there is a charging opportunity and the constraints (7d) and (7f) are not active; then

$$\boldsymbol{P}_c^* = \boldsymbol{T}^*\omega + P_{\text{loss}}(\boldsymbol{T}^*) + P_a - P_b(\boldsymbol{i}^*, \boldsymbol{n}^*)$$
$$\left(\frac{\partial \mathcal{H}}{\partial \boldsymbol{i}}\right)^* = -\frac{w_c}{\eta}\left(V - \frac{2R}{\boldsymbol{n}^*}\boldsymbol{i}^*\right) - \boldsymbol{\lambda}^* V = 0$$

which gives the expression for $\boldsymbol{\lambda}^*$ exactly as in (19).

Appendix C
Dynamic Programming

DP uses Bellman's principle of optimality [7] to solve the problem via backward recursion handling nonlinearities and constraints in a straightforward way. The problem of battery sizing is solved by running DP at gridded values of the battery size. For each grid value $\boldsymbol{n}_j \in \mathcal{N}$, the algorithm finds the optimal power split that minimizes the operational cost as follows:

$$J_{\text{DP}}^*\left(\boldsymbol{E}(t_k), t_k\right) = \min_{\boldsymbol{i}(t_k)}\left\{\int_{t_k}^{t_{k+1}} J\left(\boldsymbol{i}(t)\right)dt + J_{\text{DP}}^*\left(\boldsymbol{E}(t_{k+1}), t_{k+1}\right)\right\}$$
$$t_k \in \mathcal{T}; \quad \boldsymbol{i}(t_k) \in \mathcal{U}; \quad \boldsymbol{E}(t_k) \in \mathcal{X}; \quad t_k \in \mathcal{T}$$

where t_k and t_{k+1} are consecutive time instances, and $J_{\text{DP}}^*(\boldsymbol{E}(t_k), t_k)$ is a cost matrix holding the optimal cost-to-go from state $\boldsymbol{E}(t_k)$ at time t_k to the desired final state at time t_f. Sets $\mathcal{N}$, $\mathcal{T}$, $\mathcal{X}$, and $\mathcal{U}$ are discrete, and the grid resolution determines the accuracy of the solution. Hence, to obtain an accurate solution, both the state and the current are gridded with 2000 points.

The operational cost $J(\boldsymbol{i}(t))$ is computed as in (6) but with $\boldsymbol{i}(t)$ as a single control variable. Note that, for a fixed battery size, the same procedure can be applied as in Appendix B to decrease the number of control variables. Moreover, the need for $\boldsymbol{P}_c(t)$ as a control variable in (16) can also be eliminated because the EGU will be turned on only if the vehicle cannot satisfy the driving demands by the electric grid alone.

The optimization is subject to the same constraints as in (7), except the constraint for ending at the desired SOC value (7i), which is formulated as a soft constraint, i.e.,

$$J_{\text{DP}}^*\left(\boldsymbol{E}(t_f), t_f\right) = 1000\left|\boldsymbol{E}(t_f) - \text{soc}_0 QV\boldsymbol{n}_j\right|.$$

The infeasible points in $J_{\text{DP}}^*(\boldsymbol{E}(t_k), t_k)$ have been given a cost of 1000 and the sampling time is 1 s.

Appendix D
Convex Subproblem: CS

The convex subproblem (7), where $\boldsymbol{e}(t)$ is not a decision variable, can be written in discrete time as

minimize

$$h\sum_{0}^{N-1} J\left(\boldsymbol{P}_g(k), \boldsymbol{P}_c(k), e(k)\right) + w_b\boldsymbol{n}$$

subject to, $\forall k \in \{0, \ldots, N-1\}$

$$\boldsymbol{T}(k) \geq \max\left\{T_{\min}\left(\omega(k)\right), T_v(\boldsymbol{n}, k)\right\}$$
$$\boldsymbol{T}(k)\omega(k) + P_{\text{loss}}\left(\boldsymbol{T}(k), k\right) \leq P_b\left(\boldsymbol{i}(k), \boldsymbol{n}\right) + \boldsymbol{P}_g(k)e(k) + \boldsymbol{P}_c(k)c(k) - P_a$$
$$\boldsymbol{i}(k) \in [i_{c,\min}, i_{c,\max}]\boldsymbol{n}$$
$$\boldsymbol{P}_g(k) \in [0, P_{g,\max}]$$
$$\boldsymbol{P}_c(k) \in [0, \eta P_{c,\max}]$$
$$\boldsymbol{E}(k+1) = \boldsymbol{E}(k) - hV\boldsymbol{i}(k)$$
$$\boldsymbol{E}(k) \in [\text{soc}_{\min}, \text{soc}_{\max}]QV\boldsymbol{n}$$
$$\boldsymbol{E}(N) = \boldsymbol{E}(0) = \text{soc}_0 QV\boldsymbol{n}$$
$$\boldsymbol{n} > 0$$

where h is the sampling time, and N is the total number of samples.

The decision variables are scaled and a parser is used, i.e., CVX [31], to translate the problem into a form required by the solver SeDuMi [22].

Acknowledgment

The authors would like to thank Chalmers Center for Computational Science and Engineering (C3SE), where the DP computations were performed.

REFERENCES

[1] L. Guzzella and A. Sciarretta, *Vehicle Propulsion Systems, Introduction to Modeling and Optimization*, 2nd ed. Berlin, Germany: Springer-Verlag, 2007.

[2] "AutoTram: Transport System of the Future," Dresden, Germany, Tech. Rep., 2010.

[3] "On-Line Electric Vehicle," Daejeon, Korea, Tech. Rep., 2009.

[4] M. Johansson and O. Olsson, "Feasibility study of dual-mode buses in Gothenburg's public transport," M.S. thesis, Dept. Technol. Manage. Econom., Chalmers Univ. of Technol., Gothenburg, Sweden, 2011.

[5] L. Johannesson, S. Pettersson, and B. Egardt, "Predictive energy management of a 4QT series-parallel hybrid electric bus," *Control Eng. Practice*, vol. 17, no. 12, pp. 1440–1453, Dec. 2009.

[6] T. C. Moore, "HEV control strategy: Implications of performance criteria, system configuration and design, and component selection," in *Proc. Amer. Control Conf.*, Albuquerque, NM, USA, Jun. 1997, pp. 679–683.

[7] R. Bellman, *Dynamic Programming*. Princeton, NJ, USA: Princeton Univ. Press, Jun. 1957.

[8] U. Zoelch and D. Schroeder, "Dynamic optimization method for design and rating of the components of a hybrid vehicle," Int. J. Veh. Design, vol. 19, no. 1, pp. 1–13, 1998. [Online]. Available: http://trid.trb.org/view/1998/C/476786

[9] M. Kim and H. Peng, "Power management and design optimization of fuel cell/battery hybrid vehicles," *J. Power Sources*, vol. 165, no. 2, pp. 819–832, Mar. 2007.

[10] O. Sundström, L. Guzzella, and P. Soltic, "Torque-assist hybrid electric powertrain sizing: From optimal control towards a sizing law," *IEEE Trans. Control Syst. Technol.*, vol. 18, no. 4, pp. 837–849, Jul. 2010.

[11] M. Kim and H. Peng, "Combined control/plant optimization of fuel cell hybrid vehicles," in *Proc. Amer. Control Conf.*, Minneapolis, MN, USA, Jun. 14–16, 2006, pp. 496–501.

[12] S. J. Moura, D. S. Callaway, H. K. Fathy, and J. L. Stein, "Tradeoffs between battery energy capacity and stochastic optimal power management in plug-in hybrid electric vehicles," *J. Power Sources*, vol. 195, no. 9, pp. 2979–2988, May 2010.

[13] N. Murgovski, J. Sjöberg, and J. Fredriksson, "A methodology and a tool for evaluating hybrid electric powertrain configurations," *Int. J. Elect. Hybrid Veh.*, vol. 3, no. 3, pp. 219–245, Nov. 2011.

[14] E. D. Tate and S. P. Boyd, "Finding ultimate limits of performance for hybrid electric vehicles," presented at the Soc. Autom. Eng. Future Transp. Technol. Conf., Costa Mesa, CA, USA, 2000, SAE Tech. Paper 2000-01-3099.

[15] N. Murgovski, L. Johannesson, J. Sjöberg, and B. Egardt, "Component sizing of a plug-in hybrid electric powertrain via convex optimization," *J. Mechatron.*, vol. 22, no. 1, pp. 106–120, Feb. 2012.

[16] S. Boyd and L. Vandenberghe, *Convex Optimization*. Cambridge, U.K.: Cambridge Univ. Press, 2004.

[17] L. S. Pontryagin, V. G. Boltyanskii, R. V. Gamkrelidze, and E. F. Mishchenko, *The Mathematical Theory of Optimal Processes*, L. W. Neustadt, Ed. New York, NY, USA: Interscience, 1962.

[18] W. R. Hamilton, "On a general method in dynamics," Philos. Trans. R. Soc., vol. 2, pp. 247–308, Jan. 1834. [Online]. Available: http://www.emis.de/classics/Hamilton/

[19] W. R. Hamilton, "Second essay on a general method in dynamics," Philos. Trans. R. Soc., vol. 1, pp. 95–144, Jan. 1835. [Online]. Available: http://www.emis.de/classics/Hamilton/

[20] N. Murgovski, L. Johannesson, and J. Sjöberg, "Convex modeling of energy buffers in power control applications," in *Proc. IFAC Workshop Eng. Powertrain E-CoSM*, Rueil-Malmaison, France, Oct. 23–25, 2012, pp. 92–99.

[21] S. Sager, "Reformulations and algorithms for the optimization of switching decisions in nonlinear optimal control," *J. Process Control*, vol. 19, no. 8, pp. 1238–1247, Sep. 2009.

[22] Y. Labit, D. Peaucelle, and D. Henrion, "SeDuMi interface 1.02: A tool for solving LMI problems with SeDuMi," in *Proc. IEEE Int. Symp. Comput. Aided Control Syst. Design*, Sep. 2002, pp. 272–277.

[23] G. A. Bliss, "The problem of Lagrange in the calculus of variations," *Amer. J. Math.*, vol. 52, no. 4, pp. 673–744, Oct. 1930.

[24] E. J. McShane, "On multipliers for Lagrange problems," *Amer. J. Math.*, vol. 61, no. 4, pp. 809–819, Oct. 1939.

[25] G. Paganelli, S. Delprat, T. M. Guerra, J. Rimaux, and J. Santin, "Control development for a hybrid-electric sport-utility vehicle: strategy, implementation and field test results," in *Proc. Amer. Control Conf.*, 2001, pp. 5064–5069.

[26] G. Paganelli, S. Delprat, T. M. Guerra, J. Rimaux, and J. Santin, "Equivalent consumption minimization strategy for parallel hybrid powertrains," in *Proc. IEEE Veh. Technol. Conf.*, 2002, pp. 2076–2081.

[27] A. E. Bryson and Y.-C. Ho, *Applied Optimal Control*. New York, NY, USA: Taylor & Francis, 1975.

[28] O. Sundström, D. Ambühl, and L. Guzzella, "On implementation of Dynamic Programming for optimal control problems with final state constraints," *Oil Gas Sci. Technol.*, vol. 65, no. 1, pp. 91–102, Feb. 2009.

[29] N. Murgovski, L. Johannesson, A. Grauers, and J. Sjöberg, "Dimensioning and control of a thermally constrained double buffer plug-in hev powertrain," in *Proc. 51st IEEE Conf. Decision Control*, Maui, HI, USA, Dec. 10–13, 2012, pp. 6346–6351.

[30] S. Delprat, J. Lauber, T. M. Guerra, and J. Rimaux, "Control of a parallel hybrid powertrain: Optimal control," *IEEE Trans. Veh. Technol.*, vol. 53, no. 3, pp. 872–881, May 2004.

[31] M.Grant and S. Boyd, CVX: Matlab software for disciplined convex programming 1.21 CVX Res., Inc., May 2010. [Online]. Available: http://cvxr.com/cvx

Nikolce Murgovski received the M.Sc. degree in software engineering from University West, Trollhättan, Sweden, in 2007 and the M.Sc. degree in applied physics and the Ph.D. degree in signals and systems from Chalmers University of Technology, Gothenburg, Sweden, in 2007 and 2012, respectively.

He is currently a Postdoctoral Researcher with the Department of Signals and Systems, Chalmers University of Technology. His research interests include optimal control and dimensioning of automotive powertrains.

Lars Mårdh Johannesson (M'12) received the M.Sc. degree in automation and mechatronics and the Ph.D. degree in automatic control from Chalmers University of Technology, Gothenburg, Sweden, in 2004 and 2009, respectively.

Since 2011, he has been with the Electromobility Group, Viktoria Swedish ICT, Gothenburg, working on powertrain control within the Chalmers Energy Initiative. His main research interests include optimal control of hybrid and plug-in hybrid electric vehicles, control of auxiliary systems in trucks, active cell balancing, and system studies of hybrid vehicles.

Jonas Sjöberg (M'96) received the M.Sc. degree in applied physics from Uppsala University, Uppsala, Sweden, in 1989 and the Ph.D. degree in automatic control from Linköping University, Linköping, Sweden, in 1995.

Since July 2000, he has been a Professor of mechatronics with the Department of Signals and Systems, Chalmers University of Technology, Gothenburg, Sweden. His research interests include modeling and simulation of dynamic systems based on physical insights and black-box methods based on statistics and measured data.

Dr. Sjöberg received the Volvo Cars Technology Award in 2011.